


Session 4 Paper 6	IGHEM 2008 – MILANO 3rd-6th September International Conference on Hydraulic Efficiency Measurements	 <p>2008 Milano, ITALY INTERNATIONAL GROUP FOR IGHEM HYDRAULIC EFFICIENCY MEASUREMENTS</p>
------------------------------------	--	---

Presentation of optimized integration methods and weighting corrections for the acoustic discharge measurement

Thomas Tresch
thomas.tresch@hslu.ch

Bruno Lüscher
bruno.luescher@hslu.ch

Thomas Staubli
thomas.staubli@hslu.ch

Peter Gruber
peter.gruber@rittmeyer.com

Lucerne University of Applied Sciences and Arts
Technikumstrasse 21, CH-6048 Horw, Switzerland

Rittmeyer Ltd
CH - 6340 Baar, Switzerland

Abstract

According to the appendix of the IEC 60041 standard the volume flux Q in a conduit can be determined with the acoustic discharge measurement method by integrating averaged individual path velocity readings. This is done by applying a simplified *Gauss-Jacobi* integration method, where the individual path readings are weighted and added up. This integration method is then summarized for circular and rectangular sections. The IEC 60041 has the following limitations:

First, by assuming a uniform velocity profile, the method cannot cope well with truly turbulent velocity profiles, which fall off at the boundary layers near the wall. To overcome this limitation Voser [3] proposed a modified integration method called OWICS (Optimal Weighted Integration for Circular Sections) with slightly modified optimum sensor positions and weighting coefficients, thus reducing the integration error by 0.1 up to 0.2 percent.

Second, the method uses fixed weighting of the averaged path velocities and thus the need for very accurate positioning of the acoustic transducers with respect to the prescribed distances d_i of the acoustic paths to the pipe centre. Voser [3] also suggested to include the actual, measured path positions for determination of the weighting coefficients and hereby reducing the positioning error strongly.

Third, the method is only documented for 4-path configurations in one or two crossed planes.

In this paper the following issues are presented in a compact way:

- 1) General formula for determining the positions and weighting for rectangular and circular cross sections. This includes for both cases uniform and turbulent velocity profiles for a varying number of paths from two to nine. The numerical values are also given in a table.
- 2) The correction formula for the modified weighting for all cases is derived in a generic way, allowing to apply the correction for an arbitrary number of paths.
- 3) Simulations show the improvement for different configurations for a selected number of malpositioned acoustic paths.

1. Multipath Acoustic Discharge Measurement

The multipath acoustic discharge measurement (ADM) is a well established method for accurate discharge measurement, especially for large closed conduits and rectangular channels.

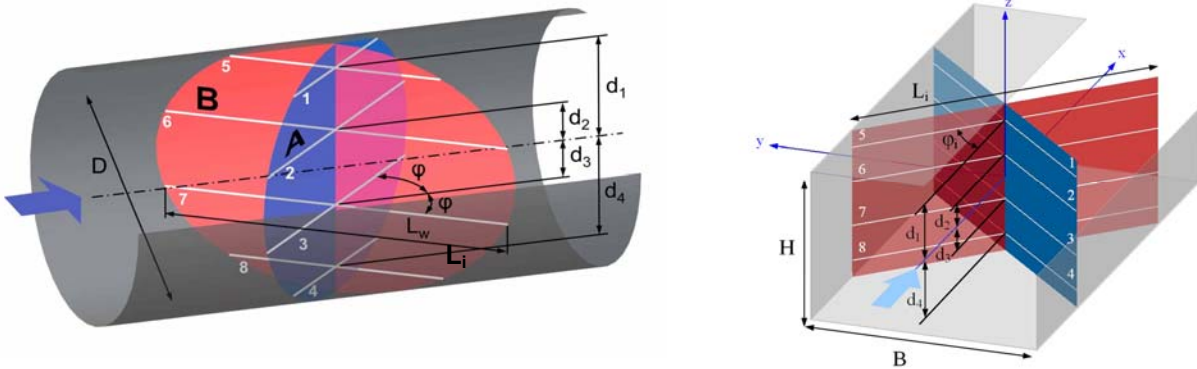


Fig. 1.1: Measurement section of an 4 path and two planes ADM for circular and rectangular sections

Figure 1 show typical 2x4-path applications in two planes for a closed conduit. The two planes allow compensation of cross flows effects in the measurement section. The resulting flow rate Q is given by $Q = (Q_A + Q_B)/2$.

Averaged axial velocities $\bar{v}_{ax,1}, \dots, \bar{v}_{ax,N}$ are measured on each of the acoustic paths. These path velocities are influenced by local flow disturbances and possible cross flow in the measuring section. The volume flux in the entire cross section is estimated by averaging and weighting dependent on the integration method the individual path readings. The theoretical achievable accuracy of this flow measuring method increases with larger pipe diameters, higher velocities and a higher number of paths.

The following sections unify the different integration methods by introducing a general form of the so called aerea flow function. Further focus lies on the influence of inaccuracies of sensor positions and on the presentation of the general correction formula for the weights in order to eliminate these negative influences on the flow determination.

Without loss of generality we restrict ourselves only to non crossed path configurations. A general shape of cross section of a pipe at the measuring position is displayed in Fig. 1.1.

2. Theory of the numerical discharge integration

This section is just a brief overview of the numerical discharge measurement. For more details see Tresch & al [1]. The figure 2.1 shows a block diagram with all the required steps for the calculation of the discharge.

2.1. The area flow function

If the averaged axial velocities $\bar{v}_{ax,i}$ (from ADM) were known at each height z , the discharge Q could be computed as follows:

$$Q = \int_c^d \bar{v}_{ax}(z) b(z) dz = \int_c^d F(z) dz \quad (2.1)$$

Where $F(z)$ is the area flow function and has the dimension [m²/s]. Q corresponds to the true discharge if all measurement installation and cross flow errors are neglected. Important to note is the fact, that equation (2.1) holds for any shape of the cross flow section. In multipath ADM one plane configurations N averaged axial path velocities are known at certain heights z_i , $i=1, \dots, N$, only, where N is the number of paths in one plane.

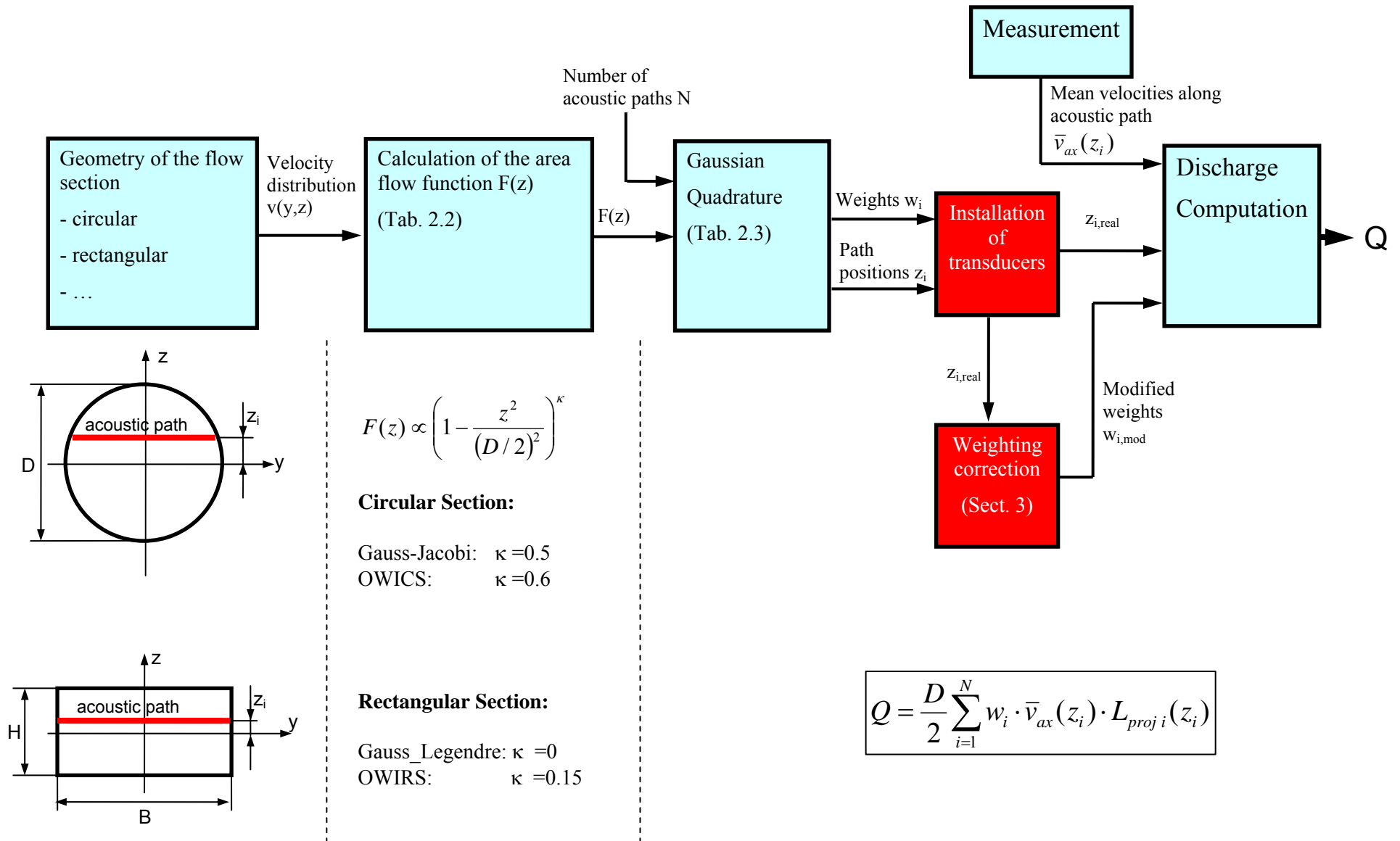


Fig. 2.1: Block diagram of the discharge computation

The basic idea of the numerical volume flux integration is therefore to approximate the integral by a weighted sum of the given real area flow function F_{real} at certain heights z_i . The real area flow function F_{real} is thus just known at the N positions where the averaged axial velocities are measured. The real area flow function $F_{real}(z)$ is supposed to be up to a certain residual term $R(z)$ close to the assumed area flow function $F(z)$:

$$F_{real}(z) = F(z)R(z) \quad (2.2)$$

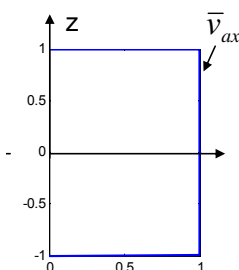
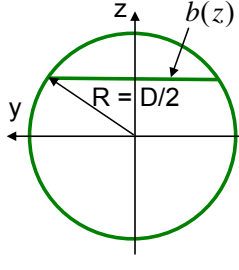
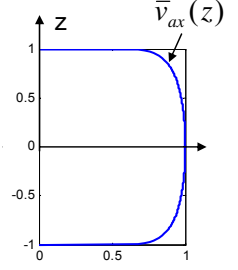
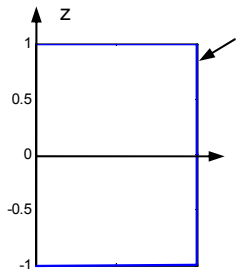
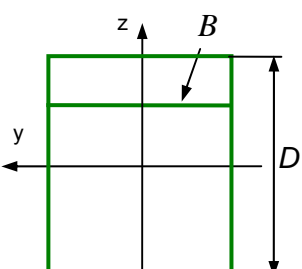
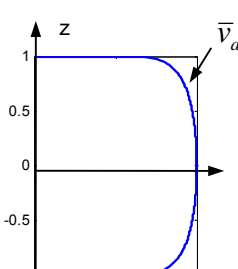
The real discharge can then be approximated as follows:

$$Q_{real} = \int_c^d F_{real}(z) dz = \int_c^d F(z)R(z) dz \cong \frac{D}{2} \sum_{i=1}^N w_i F_{real}(z_i) = \frac{D}{2} \sum_{i=1}^N w_i b(z_i) \bar{v}_{ax}(z_i) \quad (2.3)$$

In Tab. 2.2 different area flow functions $F(z)$ are summarized which correspond to the four cases:

- 1) circular section Gauss-Jacobi (IEC 60041)
- 2) circular section OWICS (Optimized Weights for Circular Section)
- 3) rectangular section Gauss Legendre (IEC 60041)
- 4) rectangular Section OWIRS (Optimized Weightings for Rectangular Sections)

Other section shapes like elliptical or egg-shaped could also be considered.

Circular sections (Tresch & al [1])		
Gauss-Jacobi (IEC 60041) 		OWICS 
$F(z) = \bar{v}_{ax} \cdot b(z)$ $F(z) = \bar{v}_{ax} \cdot D \cdot \left(1 - \frac{z^2}{(D/2)^2}\right)^{0.5}$		$F(z) = \bar{v}_{ax}(z) \cdot b(z)$ $F(z) = v_{max} \cdot D \cdot \left(1 - \frac{z^2}{(D/2)^2}\right)^{0.6}$
Rectangular sections (Lüscher & al [2])		
Gauss-Legendre (IEC 60041) 		OWIRS 
$F(z) = \bar{v}_{ax} \cdot B$ $F(z) = \bar{v}_{ax} \cdot B \cdot \left(1 - \frac{z^2}{(D/2)^2}\right)^0$		$F(z) = \bar{v}_{ax}(z) \cdot B$ $F(z) = v_{max} \cdot B \cdot \left(1 - \frac{z^2}{(D/2)^2}\right)^{0.15}$

Tab. 2.2: Summary of the area flow functions $F(z)$ for the circular and rectangular sections

As a result of the above consideration, the different area flow functions can generally be written as:

$$F(z, \kappa) \propto \left(1 - \frac{z^2}{(D/2)^2}\right)^\kappa \quad (2.4)$$

with the following values for the parameter κ :

Gauss-Jacobi:	$\kappa = 0.5$
OWICS:	$\kappa = 0.6$
Gauss_Legendre:	$\kappa = 0$
OWIRS:	$\kappa = 0.15$

2.2. Calculation of the positions and weights

For a given number of path N the *Gaussian quadrature integration method* [5] gives z_i and w_i such that the error between the real discharge Q_{real} and its approximation using the measured axial velocities only, is minimized. The theory states that the approximation of the integral is perfect for error terms $e(z)$ that can be represented by polynomials up to degree $2N-1$. That means by increasing the number of paths more disturbed profiles represented by higher order polynomials can be integrated without error.

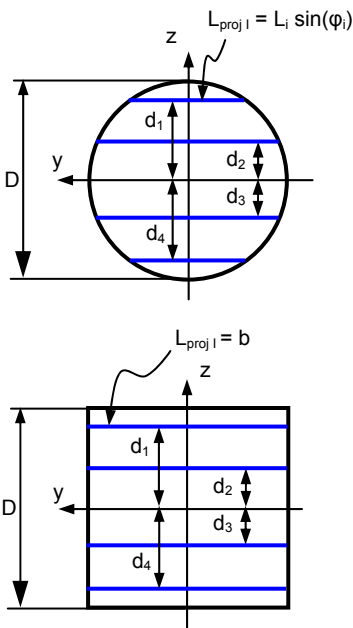
The detailed procedure of how to compute the positions and the weights are summarized in Tab. 2.3. $F(z)$ corresponds to the weight function $W(z)$ as it was introduced in Preuss [5]. The nice fact about this theory is that it holds for many different kind of functions $F(z)$ as long as the integrals given in Tab. 2.3 can be evaluated.

Computation of the path positions	Computation of the weights
<p>Polynomials are generated based on the recurrence</p> <p>$p_{-1} = 0$ $p_0 = 1$ $p_{j+1}(z) = (z - a_j) \cdot p_j(z) - b_j \cdot p_{j-1}(z) \quad (j = 0, 1, \dots, N-1)$</p> <p>where</p> $a_j = \frac{\int_a^b F(z) \cdot z \cdot p_j^2(z) \cdot dz}{\int_a^b F(z) \cdot p_j^2(z) \cdot dz}$ $b_j = \frac{\int_a^b F(z) \cdot p_j^2(z) \cdot dz}{\int_a^b F(z) \cdot p_{j-1}^2(z) \cdot dz} \quad (j = 1, 2, \dots, N)$ <p>The path positions z_1, z_2, \dots, z_N of the N-point numerical integration are equal to the roots (zeros) of the polynomial $p_N(z)$ generated by the recurrence.</p>	$w_j = \frac{1}{F(z_j)} \int_a^b F(z) \cdot L_j(z) \cdot dz \quad (j = 1, 2, \dots, N) \quad (2.5)$ <p>where $L_j(z)$ is the j'th Lagrange Polynomial:</p> $L_j(z) = \prod_{\substack{k=0 \\ k \neq j}}^N \frac{z - z_k}{z_j - z_k} \quad (2.6)$ <p>with the path positions z_1, z_2, \dots, z_N</p> <p>In these computations $F(z)$ is the assumed area flow function</p>

Tab. 2.3: Formulas for the computation of the positions and the weights, from [1].

The complete list of all relevant cases is shown in Tab. 2.4. As the number of paths is a design parameter dependent on the difficulty of the hydraulic conditions at the measuring cross section, the list includes all arrangement up to 9 path (18 crossed paths).

$$Q = \frac{D}{2} \sum_{i=1}^N w_i \cdot \bar{v}_{axi} \cdot L_{proj i}$$



Number of paths N	Gauss-Jacobi		OWICS		Gauss-Legendre		OWIRS	
	Positions d/(D/2)	Weights wi	Positions d/(D/2)	Weights wi	Positions d/(D/2)	Weights wi	Positions d/(D/2)	Weights wi
1	0	1.570796	0	1.513365	0	2	0	1.837286
2	0.5	0.906900	0.487950	0.890786	0.577350	1	0.550482	0.969761
3	0 0.707107	0.785398 0.555360	0 0.695608	0.768693 0.553707	0 0.774597	0.888889 0.555556	0 0.752355	0.853688 0.557403
4	0.309017 0.809017	0.597566 0.369316	0.303783 0.799639	0.588228 0.371884	0.339981 0.861136	0.652145 0.347855	0.329729 0.844510	0.634200 0.356143
5	0 0.5 0.866025	0.523599 0.453450 0.261799	0 0.493266 0.858534	0.515768 0.448857 0.265433	0 0.538469 0.906180	0.568889 0.478629 0.236927	0 0.525989 0.893646	0.554092 0.470657 0.245772
6	0.222521 0.623490 0.909969	0.437547 0.350885 0.194727	0.219676 0.616712 0.894939	0.432160 0.348913 0.198413	0.238619 0.661209 0.932470	0.467914 0.360762 0.171324	0.233427 0.649158 0.922789	0.458140 0.357811 0.179346
7	0 0.382683 0.707107 0.923880	0.392699 0.362807 0.277680 0.150279	0 0.378515 0.700797 0.918958	0.388174 0.359341 0.277122 0.153701	0 0.405845 0.741531 0.949108	0.417959 0.381830 0.279705 0.129485	0 0.398454 0.730661 0.941444	0.409876 0.375801 0.279255 0.136455
8	0.173648 0.5 0.766044 0.939693	0.343763 0.302300 0.224375 0.119388	0.171873 0.495335 0.760344 0.935615	0.340324 0.300163 0.224578 0.122463	0.183435 0.525532 0.796666 0.960290	0.362684 0.313707 0.222381 0.101229	0.180326 0.517455 0.787085 0.954089	0.356680 0.310151 0.223172 0.107221
9	0 0.309017 0.587785 0.809017 0.951057	0.314159 0.298783 0.254160 0.184658 0.097081	0 0.306222 0.583053 0.803925 0.947631	0.311216 0.296281 0.252911 0.185265 0.099815	0 0.324253 0.613371 0.836031 0.968160	0.330239 0.312347 0.260611 0.180648 0.081274	0 0.319446 0.605335 0.827640 0.963048	0.325159 0.308080 0.258640 0.182040 0.086431

Tab. 2.4: Complete positions and weights for multipath configuration up to the order of 9 (one plane)

3. Non-ideal path positions

For non-ideal path positions Voser [3] has given formulas for the correction of the weights for 4 acoustic paths configurations in a circular section.

It is shown here that the correction formulas for the weights can be generated from equations (2.5) and (2.6) in a generic way for arbitrary cross-sections (circular, rectangular, elliptic ...) and path numbers N.

3.1 Correction formulas for the weights

According to (2.5) the integration weights are calculated with the formula

$$w_i = \frac{1}{(1 - 4z_i^2 / D^2)^\kappa} \cdot \frac{2}{D} \cdot \int_{-D/2}^{D/2} (1 - 4z^2 / D^2)^\kappa \cdot L_i(z) dz \quad (3.1)$$

where

z_i : The actual positions of the installed acoustic paths ($i=1..N$) with $-D/2 < z_i < D/2$

D : Diameter of a circular section / Height of rectangular section

κ : Parameter dependent on the integration model

Circular-Sections: Gauss-Jacobi $\kappa=0.5$, OWICS $\kappa=0.6$

Rectangular-Sections: Gauss-Legendre $\kappa=0$, OWIRS $\kappa=0.15$

L_i : The Lagrangian-Polynomial given by

$$L_i(z) = \prod_{\substack{k=1 \\ k \neq i}}^N \frac{z - z_k}{z_i - z_k}$$

For simplicity reasons we substitute

$$z_i = x_i \cdot D / 2 \quad (-1 < z_i < 1) \quad (3.2)$$

hence formula (3.1) equals

$$w_i = \frac{1}{(1 - x_i^2)^\kappa} \int_{-1}^1 (1 - x^2)^\kappa \cdot L_i(x) dx \quad (3.3)$$

In the following the integral (3.3) is evaluated for 2, 3, .., 6 acoustic paths. Additionally it is shown, that the evaluated integrals yield a correction formula for non-ideal path positions z_i (d_i resp.).

2- Path installation:

The two weights from (3.3) in a 2-path configuration can be computed in the following way:

$$w_1 = \frac{1}{(1 - x_1^2)^\kappa} \int_{-1}^1 (1 - x^2)^\kappa \cdot L_1(x) dx = \frac{1}{(1 - x_1^2)^\kappa} \int_{-1}^1 (1 - x^2)^\kappa \cdot \frac{x - x_2}{x_1 - x_2} dx = \frac{1}{(1 - x_1^2)^\kappa \cdot (x_1 - x_2)} \left[\underbrace{\int_{-1}^1 (1 - x^2)^\kappa x dx}_{=0(\text{odd function})} - \underbrace{\int_{-1}^1 (1 - x^2)^\kappa dx}_{=g_1(\kappa)} \cdot x_2 \right]$$

$$w_1 = \frac{-g_1(\kappa) \cdot x_2}{(1 - x_1^2)^\kappa \cdot (x_1 - x_2)}$$

$$w_2 = \frac{1}{(1-x_2^2)^\kappa} \int_{-1}^1 (1-x^2)^\kappa \cdot L_2(x) dx = \frac{1}{(1-x_2^2)^\kappa} \int_{-1}^1 (1-x^2)^\kappa \cdot \frac{x-x_1}{x_2-x_1} dx = \frac{1}{(1-x_2^2)^\kappa \cdot (x_2-x_1)} \left[\underbrace{\int_{-1}^1 (1-x^2)^\kappa x dx}_{=0(\text{odd function})} - \underbrace{\int_{-1}^1 (1-x^2)^\kappa dx}_{=g_1(\kappa)} \cdot x_1 \right]$$

$$w_2 = \frac{-g_1(\kappa) \cdot x_1}{(1-x_2^2)^\kappa \cdot (x_2-x_1)}$$

Back substitution with (3.2) yields

$$w_1 = \frac{-g_1(\kappa) \cdot z_2}{(1-4z_1^2/D^2)^\kappa \cdot (z_1-z_2)} \quad w_2 = \frac{-g_1(\kappa) \cdot z_1}{(1-4z_2^2/D^2)^\kappa \cdot (z_2-z_1)}$$

Note that $z_1 > 0$ and $z_2 < 0$. To avoid mistakes the distance d_i (always positive) between the acoustic paths and the y -axis is used (see Fig. 3.1).

$$w_1 = + \frac{g_1(\kappa) \cdot d_2}{(1-4d_1^2/D^2)^\kappa \cdot (d_1+d_2)} \quad (3.4)$$

$$w_2 = + \frac{g_1(\kappa) \cdot d_1}{(1-4z_2^2/D^2)^\kappa \cdot (d_1+d_2)}$$

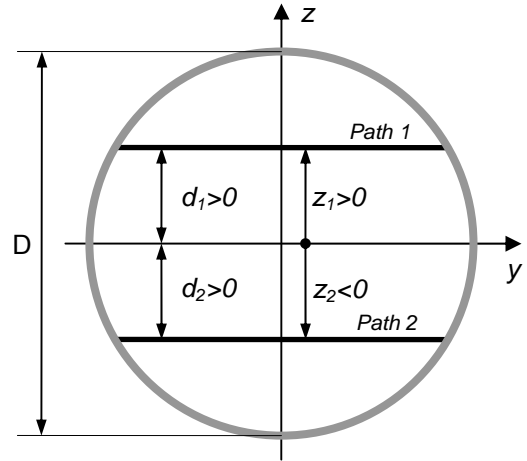


Fig. 3.1: Arrangement of a 2-path ADM

The constants $g_1(\kappa)$ for different integration methods (i.e. different values for κ) are summarized in Tab. 3.1

3-Path installation:

For three acoustic paths the same calculation as for two paths gives the following formulas for the weights:

$$w_i = \frac{g_2(\kappa) + g_1(\kappa) \cdot \prod_{\substack{k=1 \\ k \neq i}}^3 x_k}{(1-x_i^2)^\kappa \prod_{\substack{k=1 \\ k \neq i}}^3 (x_i - x_k)} \quad (i=1,2,3)$$

$$w_1 = \frac{g_2(\kappa) + g_1(\kappa) \cdot x_2 \cdot x_3}{(1-x_1^2)^\kappa (x_1 - x_2)(x_1 - x_3)}$$

$$w_2 = \frac{g_2(\kappa) + g_1(\kappa) \cdot x_1 \cdot x_3}{(1-x_2^2)^\kappa (x_2 - x_1)(x_2 - x_3)}$$

$$w_3 = \frac{g_2(\kappa) + g_1(\kappa) \cdot x_1 \cdot x_2}{(1-x_3^2)^\kappa (x_3 - x_1)(x_3 - x_2)}$$

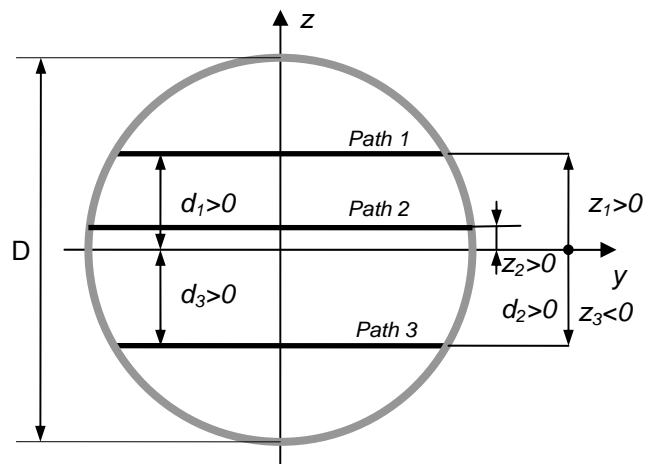


Fig. 3.2: Arrangement of a 3-path ADM

The exact position for path 2 is $z_2=0$. Therefore z_2 can always be chosen positive (due to symmetry).

After back substitution with (3.2):

$$w_1 = \frac{g_2(\kappa)D^2/4 - g_1(\kappa) \cdot d_2 \cdot d_3}{(1 - 4d_1^2/D^2)^\kappa (d_1 - d_2)(d_1 + d_3)} \quad w_2 = \frac{g_2(\kappa)D^2/4 - g_1(\kappa) \cdot d_1 \cdot d_3}{(1 - 4d_2^2/D^2)^\kappa (d_2 - d_1)(d_2 + d_3)} \quad (3.5)$$

$$w_3 = \frac{g_2(\kappa)D^2/4 + g_1(\kappa) \cdot d_1 \cdot d_2}{(1 - 4d_3^2/D^2)^\kappa (d_3 + d_1)(d_3 + d_2)}$$

4-Path installation:

$$w_i = - \frac{g_2(\kappa) \sum_{\substack{k=1 \\ k \neq i}}^4 x_k + g_1(\kappa) \prod_{\substack{k=1 \\ k \neq i}}^4 x_k}{(1 - x_i^2)^\kappa \prod_{\substack{k=1 \\ k \neq i}}^4 (x_i - x_k)} \quad (i=1, \dots, 4) \quad (3.6)$$

$$w_1 = - \frac{g_2(\kappa)(x_2 + x_3 + x_4) + g_1(\kappa) \cdot x_2 \cdot x_3 \cdot x_4}{(1 - x_1^2)^\kappa (x_1 - x_2)(x_1 - x_3)(x_1 - x_4)} \quad w_2 = - \frac{g_2(\kappa)(x_1 + x_3 + x_4) + g_1(\kappa) \cdot x_1 \cdot x_3 \cdot x_4}{(1 - x_2^2)^\kappa (x_2 - x_1)(x_2 - x_3)(x_2 - x_4)}$$

$$w_3 = - \frac{g_2(\kappa)(x_1 + x_2 + x_4) + g_1(\kappa) \cdot x_1 \cdot x_2 \cdot x_4}{(1 - x_3^2)^\kappa (x_3 - x_1)(x_3 - x_2)(x_3 - x_4)} \quad w_4 = - \frac{g_2(\kappa)(x_1 + x_2 + x_3) + g_1(\kappa) \cdot x_1 \cdot x_2 \cdot x_3}{(1 - x_4^2)^\kappa (x_4 - x_1)(x_4 - x_2)(x_4 - x_3)}$$

After back substitution (3.2):

$$w_1 = \frac{g_2(\kappa) \cdot D^2/4(d_3 + d_4 - d_2) - g_1(\kappa) \cdot d_2 \cdot d_3 \cdot d_4}{(1 - 4d_1^2/D^2)^\kappa (d_1 - d_2)(d_1 + d_3)(d_1 + d_4)} \quad w_2 = \frac{g_2(\kappa) \cdot D^2/4(d_3 + d_4 - d_1) - g_1(\kappa) \cdot d_1 \cdot d_3 \cdot d_4}{(1 - 4d_2^2/D^2)^\kappa (d_2 - d_1)(d_2 + d_3)(d_2 + d_4)}$$

$$w_3 = \frac{g_2(\kappa) \cdot D^2/4 \cdot (d_1 + d_2 - d_4) - g_1(\kappa) \cdot d_1 \cdot d_2 \cdot d_4}{(1 - 4d_3^2/D^2)^\kappa (d_1 + d_3)(d_2 + d_3)(d_3 - d_4)} \quad w_4 = \frac{g_2(\kappa) \cdot D^2/4(d_1 + d_2 - d_3) - g_1(\kappa) \cdot d_1 \cdot d_2 \cdot d_3}{(1 - 4d_4^2/D^2)^\kappa (d_1 + d_4)(d_2 + d_4)(d_4 - d_3)}$$

The above correction formulas for the 4-path installation are equal to the formulas derived by Voser [3].

5-Path installation:

$$w_i = \frac{g_3(\kappa) + g_2(\kappa) \sum_{\substack{k,j=1 \\ k < j \\ k,j \neq i}}^5 x_k \cdot x_j + g_1(\kappa) \prod_{\substack{k=1 \\ k \neq i}}^5 x_k}{(1 - x_i^2)^\kappa \prod_{\substack{k=1 \\ k \neq i}}^5 (x_i - x_k)} \quad (\text{for } i=1, \dots, 5) \quad (3.7)$$

example:

$$w_1 = \frac{g_3(\kappa) + g_2(\kappa)(x_2 \cdot x_3 + x_2 \cdot x_4 + x_2 \cdot x_5 + x_3 \cdot x_4 + x_3 \cdot x_5 + x_4 \cdot x_5) + g_1(\kappa)x_2 \cdot x_3 \cdot x_4 \cdot x_5}{(1 - x_1^2)^\kappa (x_1 - x_2)(x_1 - x_3)(x_1 - x_4)(x_1 - x_5)}$$

6-Path installation:

$$w_i = - \frac{g_3(\kappa) \sum_{\substack{k=1 \\ k \neq i}}^6 x_k + g_2(\kappa) \sum_{\substack{k,j,l=1 \\ k < j < l \\ k,j,l \neq i}}^6 x_k \cdot x_j \cdot x_l + g_1(\kappa) \prod_{\substack{k=1 \\ k \neq i}}^6 x_k}{(1-x_i^2)^\kappa \prod_{\substack{k=1 \\ k \neq i}}^6 (x_i - x_k)} \quad (\text{for } i=1,\dots,6) \quad (3.8)$$

example

$$w_1 = - \frac{g_3(\kappa)(x_2 + x_3 + x_4 + x_5 + x_6) + g_2(\kappa)(x_2x_3x_4 + x_2x_3x_5 + x_2x_3x_6 + x_2x_4x_5 + x_2x_4x_6 + x_2x_5x_6 + x_3x_4x_5 + x_3x_4x_6 + x_3x_5x_6 + x_4x_5x_6) + g_1(\kappa)x_2 \cdot x_3 \cdot x_4 \cdot x_5 \cdot x_6}{(1-x_1^2)^\kappa (x_1 - x_2)(x_1 - x_3)(x_1 - x_4)(x_1 - x_5)(x_1 - x_6)}$$

	Circular section		Rectangular section	
	Gauss-Jacobi $\kappa = 0.5$	OWICS $\kappa = 0.6$	Gauss-Legendre $\kappa = 0$	OWIRS $\kappa = 0.15$
$g_1(\kappa)$	1.570796	1.513365	2	1.837286
$g_2(\kappa)$	0.392699	0.360325	2/3	0.556753
$g_3(\kappa)$	0.196350	0.174351	2/5	0.315143

Tab. 3.1: Summary of the integration constants for the correction formulas. The calculation is based on the integral $g_i(\kappa) = \int_{-1}^1 (1-x^2)^\kappa \cdot x^{2(i-1)} dx \quad (i=1,2,3,\dots)$.

3.2 Validation of the correction formulas for circular sections

The validations for the correction formulas are based on the theoretical velocity profile $v(r)$ for a turbulent flow in a circular section given by

$$v(r) = v_{\max} \left(1 - \frac{r}{R} \right)^{1/n} \quad (3.9)$$

where m ($6 < n < 12$) is a function of the Reynolds number Re and the wall roughness k (see [4])

The following figures show the error of the measured flow rate compared to the exact flow rate for non-ideal positioned acoustic path. Three different cases are illustrated

- Error with the Gauss-Jacobi method (IEC-60041) (weights from Tab 2.4)
- Error with the modified Gauss-Jacobi method (modified weights from 3.4 - 3.8 where $\kappa=0.5$)
- Error with the modified OWICS method (modified weights from 3.4 - 3.8 where $\kappa=0.6$)

2- Path installation:

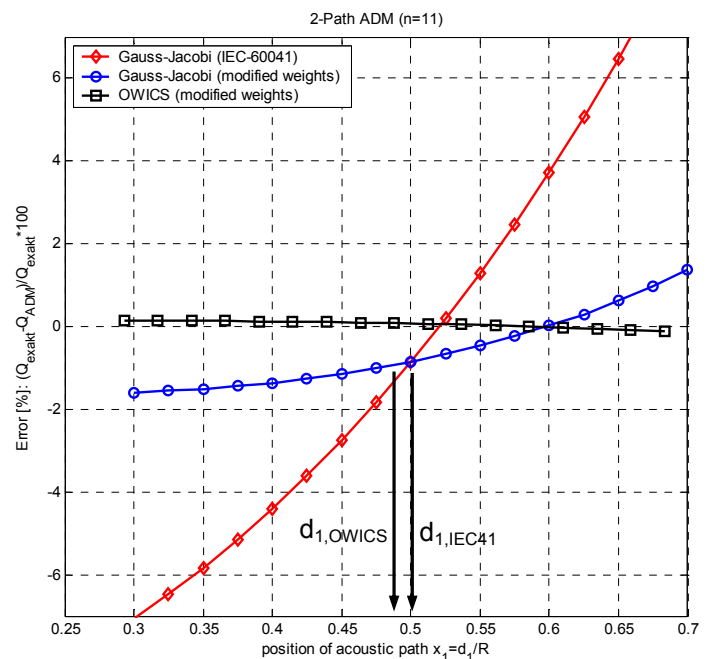
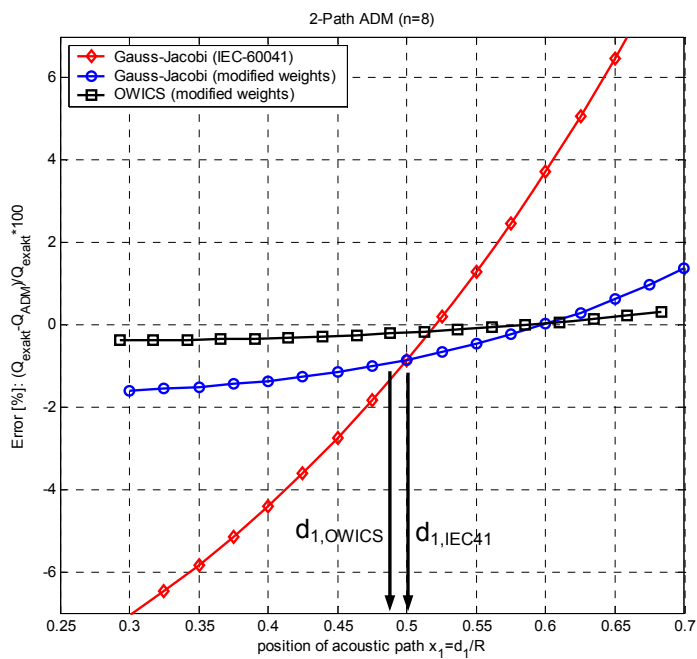
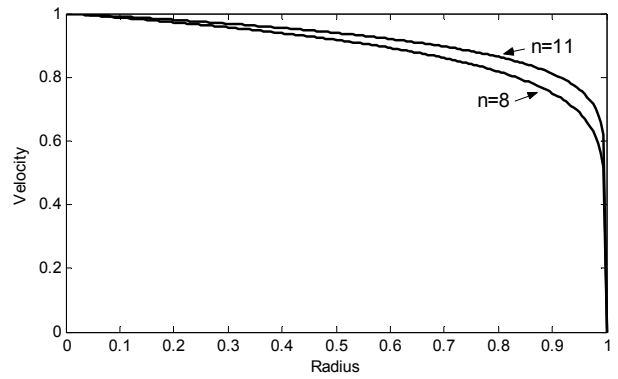
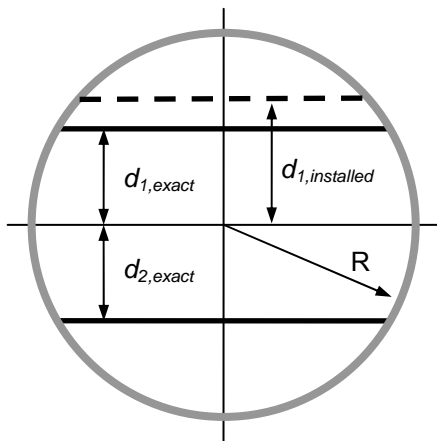


Fig. 3.3: Integration errors of non-ideal path positions with two different velocity profiles

3- Path installation:

case 1: position of path 1 is non-ideal

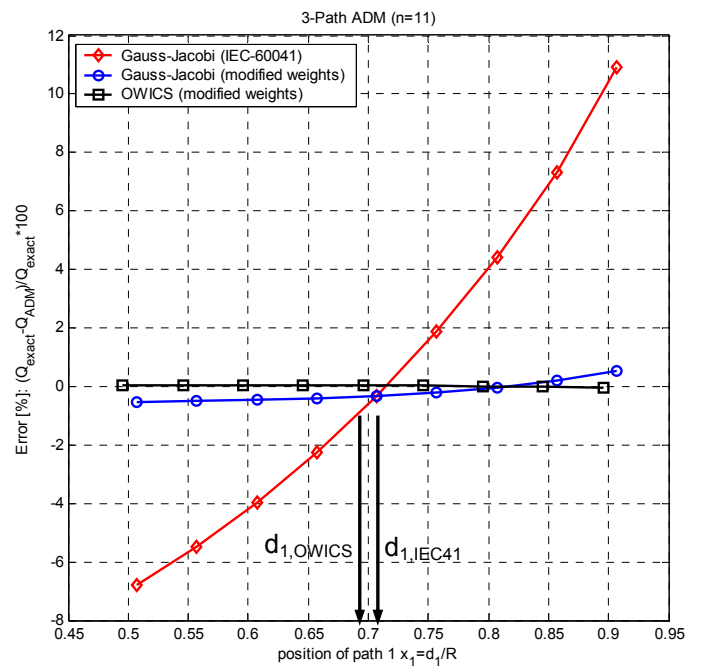
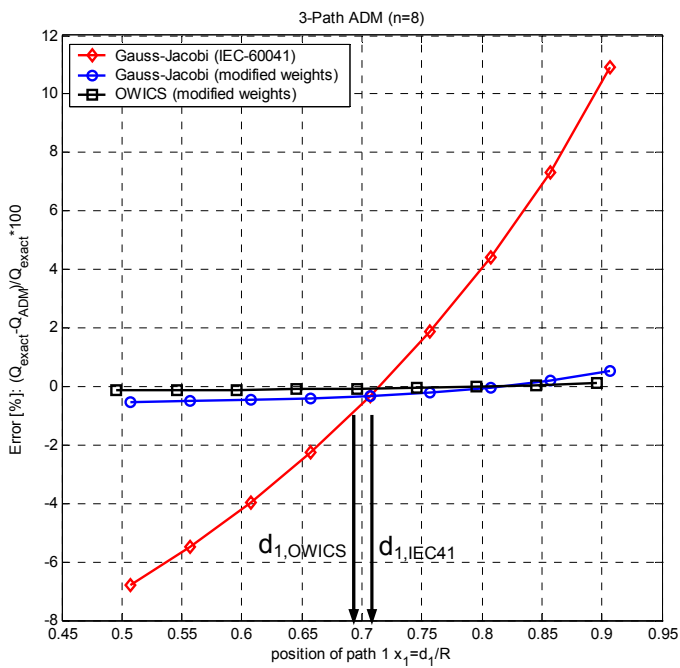
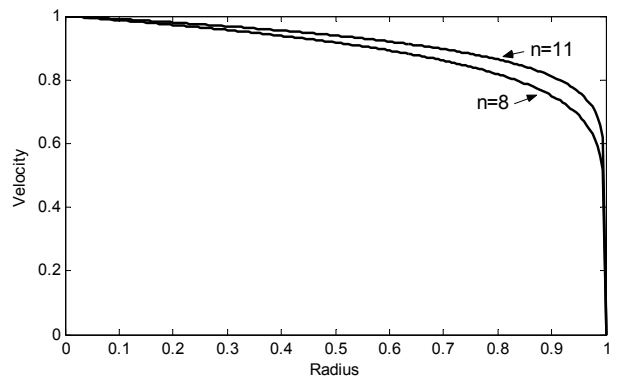
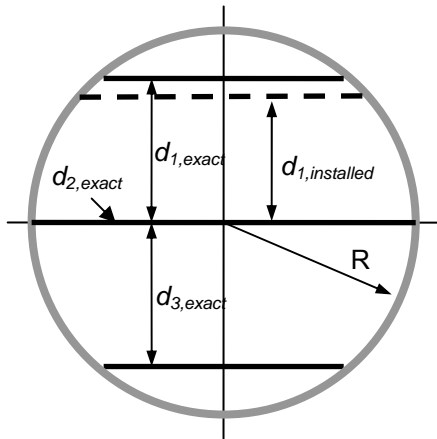


Fig. 3.4: Integration errors of non-ideal path positions with two different velocity profiles

case 2: position of path 2 is non-ideal

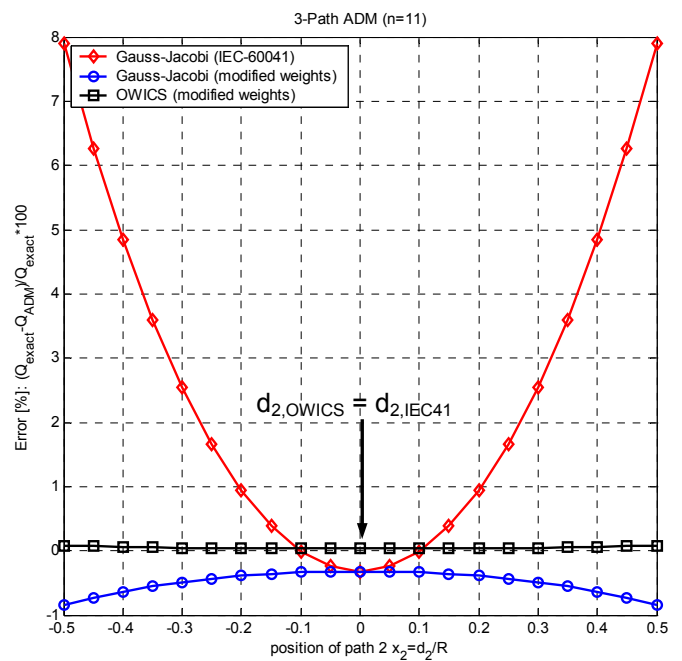
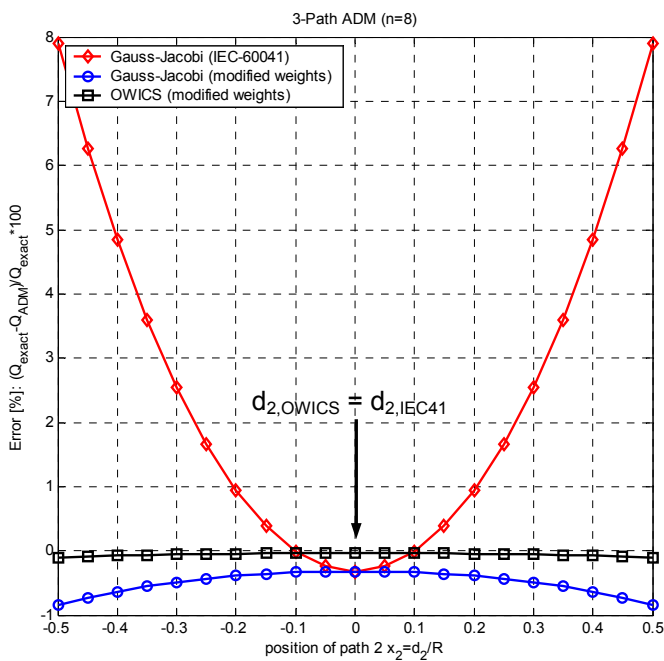
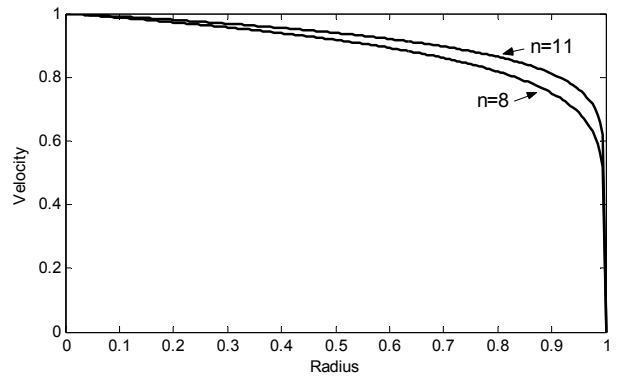
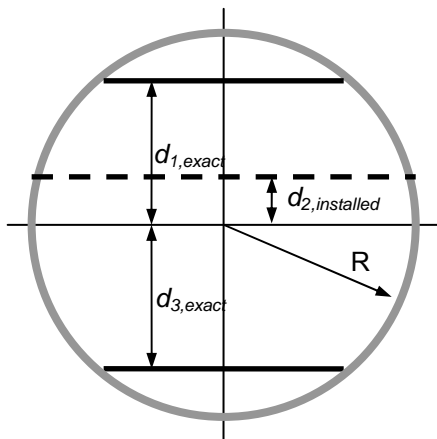


Fig. 3.4: Integration errors of non-ideal path positions with two different velocity profiles

The same validations for the 4-path installation have already been done (see Voser [3] and Tresch & al [1]).

Conclusion

The complete set of path positions and weights for uniform and turbulent velocity profiles contains all important multi-path applications. When dealing with turbulent velocity profiles the OWICS and OWIRS method are the most adequate.

For nonideal path positions for circular section, the simulations show that if the weights of altered positions are corrected for the Gauss-Jacobi (IEC41) and the OWICS methods, the error becomes smaller (modified Gauss Jacobi), and even almost zero for the OWICS method. In Lüscher & al [2] similar results have been found for rectangular sections.

It has however not yet been proven, under which exact conditions the correction formula can be applied resulting in very small integration errors. Even so an inclusion of the optimized weighting methods OWICS and OWIRS with the correction formula is strongly proposed for the IEC 60041 code.

References

1. T. Tresch, P. Gruber, T. Staubli: *Comparison of integration methods for multipath acoustic discharge measurements*, IGHEM 2006, Portland - <http://www.ighem.org/Paper2006/d6.pdf>
2. B. Lüscher, T. Staubli, T. Tresch, P. Gruber: *Optimizing the acoustic discharge measurement for rectangular conduits*, IGHEM 2008, Milano
3. Voser A.: *Analyse und Fehleroptimierung der mehrgfadigen akustischen Durchflussmessung in Wasserkraftanlagen*, ETH Zürich, Dissertation Nr. 13102, 1999
4. Nikuradse: *Untersuchungen über die Geschwindigkeitsverteilung in turbulenten Strömungen. Diss. Göttingen 1926*; VDI-Forschungsheft 281, 1926
5. W.H. Preuss, S.A. Teukolsky, W.T. Vetterling, and B.P. Flannery, *Numerical Recipes in C, 2nd edition*, Cambridge University Press, 1995. (The same book exists for the Fortran language).